# Structural Characterization and Catalytic Behavior of $Al_2O_3$-Supported Cerium Oxides

Masaaki HANEDA, Takanori MIZUSHIMA, Noriyoshi KAKUTA, Akifumi UENO, Yasunori SATO,†
Shinji MATSUURA,† Koichi KASAHARA,† and Masayasu SATO†
Department of Materials Science, Toyohashi University of Technology, Tempaku, Toyohashi, Aichi 441
† Cataler Industrial Co., Daito-cho, Ogasagun, Shizuoka 437-14

(Received October 16, 1992)

Three kinds of supported cerium oxide catalysts were prepared by an impregnation and a sol–gel technique using aluminium tri-isopropoxide (AIP) and cerium(III) nitrate dissolved in ethylene glycol. One is cerium dioxide supported on alumina, and others are finely-divided nonstoichiometric cerium oxide and cerium aluminate crystallites dispersed on alumina, respectively. In order to investigate the relationship between the structure of cerium oxides and their catalytic behavior, these cerium oxides were subjected to "OSC" (oxygen storage capacity) measurements as well as kinetic studies for methane oxidation. The highest "OSC" was achieved on the finely-divided nonstoichiometric cerium oxides. Kinetics studies for methane oxidation resulted in the first order with respect to methane for all the catalysts, and nearly zero order with respect to oxygen on the cerium dioxide and cerium aluminate. While on the finely-divided nonstoichiometric cerium oxides a half order with respect to oxygen was obtained. On the basis of these results the structure and the catalytic behavior of cerium oxides was discussed in terms of the "OSC" associated with the oxygen vacancies existed in the finely-divided nonstoichiometric cerium oxides. A brief discussion was also made on Pd catalysts supported on these cerium oxides for methane oxidation.

Because of a low redox potential between $Ce^{3+}$ and $Ce^{4+}$ (1.7 V), cerium dioxide dominates in the oxidative atmosphere, while in the reducing circumstance cerium sesquioxide becomes predominant.[1] Thus, cerium oxides can either absorb or release oxygen depending on the oxygen concentration in the gas phase; $2CeO_2 \rightleftharpoons Ce_2O_3 + 1/2O_2$. The amounts of oxygen reversibly provided into and removed from the gas phase are called "OSC" (oxygen storage capacity) of cerium oxides.[2] A high "OSC" of cerium oxides is one of the reasons why they have been effectively employed as a base component of automobile three-way catalysts.[3—5]

In order to reveal the roles of oxygen reversibly absorbed in and released from cerium oxides, a lot of extensive studies have been carried out during the oxidation of carbon monoxide and methane on noble metal catalysts supported on cerium oxides. Kummer et al.[6] reported that CO oxidation activity of $Pd/Al_2O_3$ increased with the addition of cerium oxides, while for alkane oxidations on $Pt/Al_2O_3$ the catalytic activity decreased with the addition of cerium oxides because of the formation of surface-oxidized platinum.[7] Oh and Eickel[8] reported that the CO self-inhibition was suppressed by the addition of cerium oxides to $Pt/Al_2O_3$ catalyst during CO oxidation under moderately oxidizing or net-reducing conditions. Ausen and Summers[9] reported similar results that the CO oxidation activity of $Pt/Al_2O_3$ was enhanced upon the addition of small quantities of cerium oxides, yielding partially-oxidized metals. These results seem to indicate that, by the addition of cerium oxides, some of the oxygen adsorbed and activated on noble metals are inhibited to be released into gas phase or to spill over the alumina surface. This leads to the suppression of the alkane and CO adsorption on noble metals during the reactions. The amounts of oxygen released into gas phase or spilled over the catalyst support are presumably dependent upon the "OSC" of the cerium oxides employed.

There are considerable kinds of cerium oxides between dioxide and sesquioxide, identified by X-ray diffraction.[10] Those are called nonstoichiometric cerium oxides, and their "OSC" will be somewhat different with each other. The difference in the "OSC" may have an effect upon the interaction between noble metals and the oxygen ions in cerium oxides, probably resulting in the modification of the catalytic behavior of the noble metals on cerium oxides. Little attentions have been paid, however, to the relationship between the structure and the catalytic behavior of cerium oxides, although cerium oxide itself is of potential to oxidize alkane to carbon dioxide.[11,12] In the present work, three kinds of cerium oxides, $CeO_2$, $CeO_{2-x}$ and $CeAlO_3$, were prepared and subjected to "OSC" measurements to discuss the relationship between the structure and the "OSC" of the cerium oxides in terms of the oxygen vacancies. In addition, methane oxidation on these three cerium oxides was carried out to discuss the relationship between the structure and the catalytic behavior of the cerium oxides, based on the "OSC" observed above. A brief discussion on the effects of Pd addition over the cerium oxides was carried out during methane oxidation.

## Experimental

**Preparation of Catalysts.** Cerium oxide catalysts, dispersed on alumina support, were prepared by two different methods; one is an impregnation using active alumina (BET surface area of 120 $m^2g^{-1}$) and an aqueous solution of cerium(III) nitrate; 5.05 g of $Ce(NO_3)_3 \cdot 6H_2O$ in 20 ml of distilled water. The other is a coprecipitation through

gels involving both Al and Ce ions, and the gels were prepared from a mixed solution composed of boehmite sols and cerium nitrate dissolved in ethylene glycol. The boehmite sols were obtained from AIP in the same manner as described in the previous paper.[13] Both catalysts were dried at 383 K for 24 h, followed by calcination at 773 K for 4 h. The catalysts prepared by impregnation are named fresh cat(I) and those by sol–gel method are fresh cat(A), respectively. The loadings of cerium oxides, calculated as $CeO_2$, in the catalysts were settled to be 20 wt%, corresponding to 12.9 mol%. The calcined catalysts were recalcined at 1173 K for 1 h either in the flowing $O_2$ or in the flowing $H_2$, respectively. The catalysts thus oxidized or reduced at 1173 K are designated as, for instance, oxid-cat(A) or red-cat(I), respectively, below. Supported-1.0 wt% Pd catalysts were prepared by immersing the powders of oxid-cat(I) and of red-cat(A) with aqueous solution of Pd nitrate, followed by drying and reduction at 973 K for 1 h in the flowing $H_2$. For comparison, alumina-supported 1.0 wt% Pd catalysts were also prepared by a conventional impregnation method.

**Structure of Cerium Oxides.** Structure of cerium oxides was examined by X-ray diffraction (XRD, Regakudenki, Geigerflex) using a Cu tube at 30 kV and 15 mA. Since no X-ray diffraction peaks were observed for cerium oxides in the red-cat(A), extended X-ray absorption fine structure (EXAFS) was employed to study the structure around Ce ions in the red-cat(A). The EXAFS consists of a rotating Mo anode (Rigakudenki, RU-200), operated at 10 kV and 150 mA, a Johanson cut Ge (111) crystal as a monochromator, and a germanium solid-state detector.[14] In order to collect photons over $10^6$, signals were accumulated for 100 s for a data point, and the results of several scans were added and averaged to minimized statistical noises. Analysis of EXAFS data by Fourier transforms was made as has been described previously.[15] Fluorescent spectra of the cerium ions in the red-cat(A) were measured at room temperature, using a fluorescence spectrometer (Spex Co., Fluorog-II) with an excitation wavelength of 316 nm. A fluorescent peak centered around 380 nm, originated in cerium ions, was detected with a spectral resolution of 3 nm.[16]

**"OSC" Measurements and Methane Oxidation.** "OSC" of cerium oxides in the catalysts prepared were measured at temperatures ranging from 773 to 1173 K in the same manner as described previously.[17] Catalytic activities of cerium oxides for methane oxidation were evaluated using a closed circulating reactor made of quartz, directly connected to a gas chromatography. A column packed with an active carbon was employed for the analysis of methane, CO and $CO_2$ during the reaction. Kinetic measurements were carried out at 773 K, varying the partial pressure of methane ranging 0.7—6.1 kPa with a constant partial pressure of oxygen, 5.3 kPa, and varying the partial pressure of oxygen from 0.4 to 10 kPa at a constant partial pressure of methane, 1.5 kPa. From these results, the kinetic parameters were determined assuming the following rate expression; $[\text{rate}]=kP_{CH_4}{}^{m}P_{O_2}{}^{n}$. The rate constants were estimated at temperatures ranging from 673 to 873 K, using a gas containing $CH_4 : O_2 : He = 1.5 : 5.3 : 15$ kPa, to calculate the activation energy on the various cerium oxide catalysts. In all the experimental runs, the amounts of catalysts employed were 0.5 g.

**Temperature Programmed Reduction (TPR).** In order to characterize the oxygen adsorbed on these cerium oxide catalysts at 773 K, TPR measurements were carried out, elevating the temperature up to 1253 K with a temperature rising rate of 10 K $min^{-1}$. The catalysts pretreated either in the flowing $H_2$ or in the flowing $O_2$ at 1173 K were recalcined at 773 K in the flowing $O_2$ for 1 h prior to the TPR measurements. During the measurements 10 vol% $H_2$/Ar was introduced into the reactor, where 0.2 g of the catalyst powder was placed, with a flow rate of 110 ml $min^{-1}$.

## Results

**Structure of Cerium Oxides.** X-Ray diffraction patterns of all the catalysts prepared here are shown in Fig. 1, where diffraction peaks assigned to $CeO_2$ were observed for the fresh and the oxidized cat(I) and (A), while the peaks assigned to $CeAlO_3$ were detected for the reduced cat(I). No diffraction peaks were detected, however, for the reduced cat(A). Crystallite size of $CeO_2$ in the fresh and the oxidized cat(I) and (A) was estimated by an X-ray line broadening using the Scherrer's equation for the peak at $2\theta=28.6°$, ascribed to the diffraction from $CeO_2(111)$. The size of $CeO_2$ crystallites thus calculated are given in Table 1, with the BET surface areas of the catalysts. In Fig. 2 are shown the Fourier transforms of EXAFS spectra for both oxidized and reduced cat(I) and (A), respectively. The Fourier transforms of EXAFS spectra of pure $CeO_2$ and $CeAlO_3$ are also given in Fig. 2, for comparison. No reliable signals were obtained for the reduced cat(A), al-

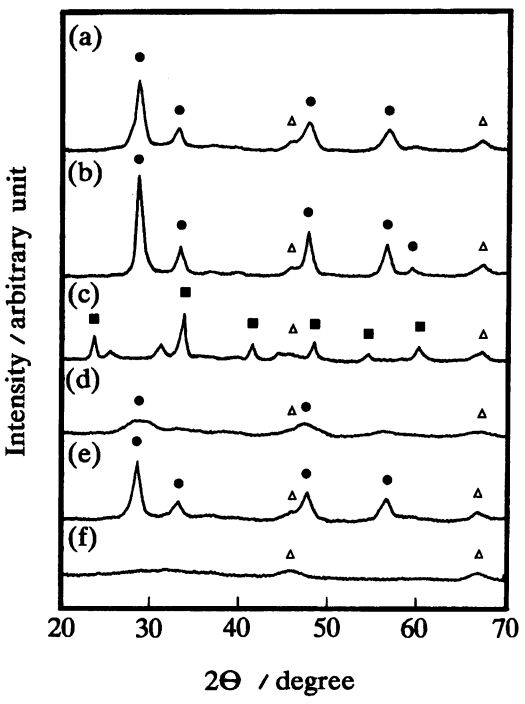


Fig. 1. XRD spectra of (a); fresh cat(I), (b); oxid-cat(I), (c); red-cat(I), (d); fresh cat(A), (e); oxid-cat(A), and (f); red-cat(A). (●) for $CeO_2$, (△) for $\gamma$-$Al_2O_3$, and (■) for $CeAlO_3$.

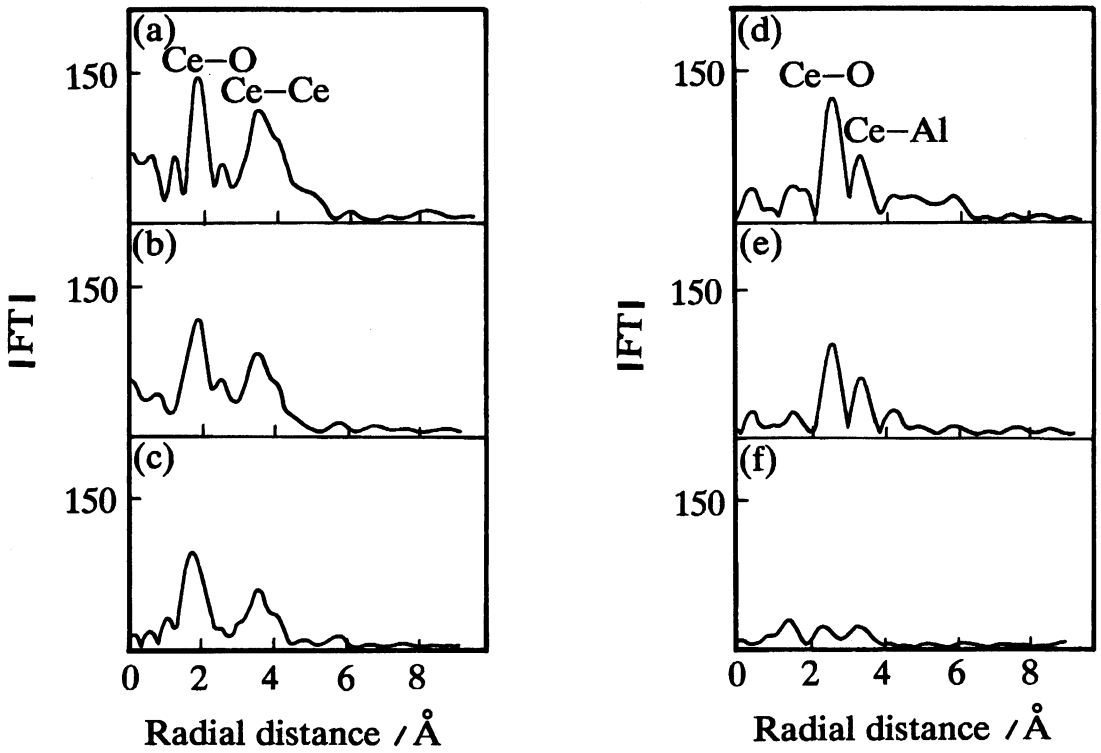


Fig. 2. Fourier transforms of EXAFS spectra: (a); pure $CeO_2$, (b); oxid-cat(I), (c); oxid-cat(A), (d); pure $CeAlO_3$, (e); red-cat(I), and (f); red-cat(A).

Table 1. Crystallite Size of $CeO_2$ and $CeAlO_3$ and the BET Surface Area of Alumina-Supported Catalysts

Crystallite size of $CeAlO_3$ was determined by X-ray line broadening method using a diffraction peak at $2\theta=33.5°$ from $CeAlO_3(110)$.

| Catalysts | Cerium oxides identified by XRD and EXAFS | Crystallite size of cerium oxides/Å | BET surface area/$m^2\ g^{-1}$ |
|---|---|---|---|
| Fresh-cat(A) | $CeO_2$ | 34 | 230 |
| Oxid-cat(A) | $CeO_2$ | 75 | 110 |
| Red-cat(A) | $CeO_{2-x}$ | — | 130 |
| Fresh-cat(I) | $CeO_2$ | 76 | 90 |
| Oxid-cat(I) | $CeO_2$ | 126 | 75 |
| Red-cat(I) | $CeAlO_3$ | 162 | 78 |

though the results obtained for the other catalysts were well consistent with the results obtained by XRD; $CeO_2$ for the oxidized cat(I) and (A), and $CeAlO_3$ for the reduced cat(I), respectively. Changes in the fluorescent intensity at 380 nm, ascribed to Ce ions in the reduced cat(A), are shown in Fig. 3, when the concentration of cerium ions, calculated as $CeO_2$, increased. A drastic depletion in the fluorescent intensity with an increase in the Ce ion concentration was observed, which is due to a concentration quenching of fluorescence.

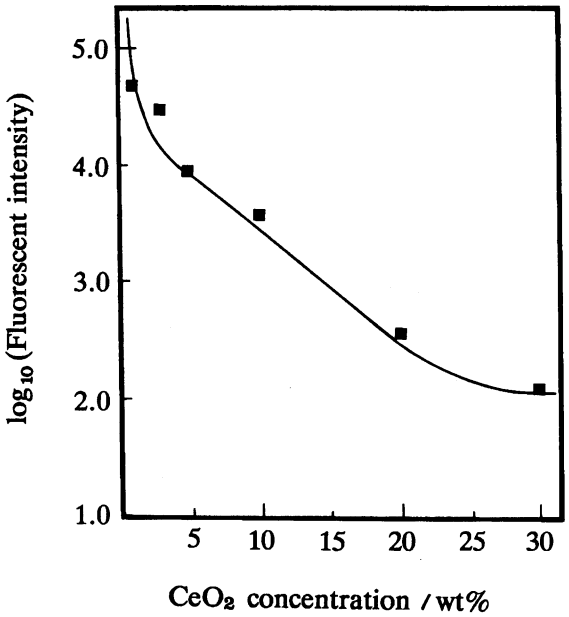


Fig. 3. Depletion of the fluorescent intensity of Ce ions in the reduced cat(A) with an increase in the Ce ion concentration.

**"OSC", Methane Oxidation, and TPR Measurements.** In Fig. 4 are illustrated the "OSC" of both oxidized and reduced cat(I) and (A), respectively, as a function of the pulsing temperature. The highest "OSC" was established with the reduced cat(A), and the "OSC" decreased in the sequence of red-cat(A)>red-cat(I)>oxid-cat(A)>oxid-cat(I). Results obtained from the kinetic studies are given in Fig. 5, where

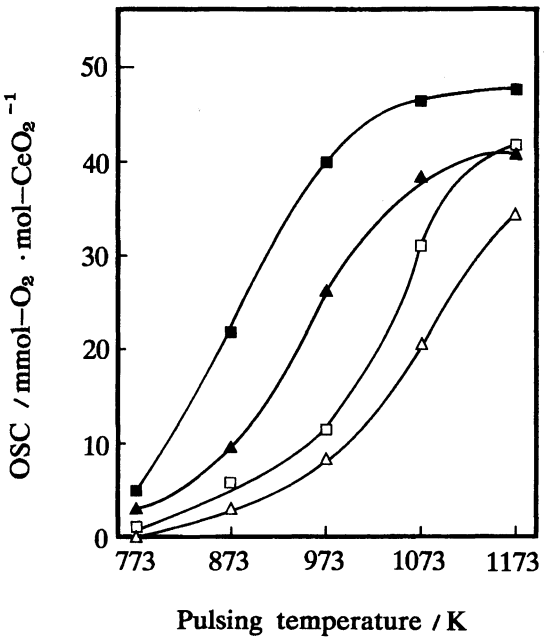


Fig. 4. Change in "OSC" with elevating temperatures. (■); red-cat(A), (▲); red-cat(I), (□); oxid-cat(A), and (△); oxid-cat(I).

either the partial pressure of methane or that of oxygen was varied at 773 K. From the results given in Fig. 5, it was found that the rates on all the catalysts, except the reduced cat(A), were independent of the partial pressure of oxygen, but increased with an increase in the partial pressure of methane so as to be described by the first order kinetics. While on the reduced cat(A), a half order with respect to oxygen and the first order with respect to methane was, however, determined (see kinetic parameters in Table 2). Change in the rate constant on these catalysts is given in Table 3, where temperatures were varied from 673 to 873 K, together with the activation energies for methane oxidation. In Fig. 6, TRP spectra of both the oxidized cat(I) and (A) are demonstrated, where the amounts of hydrogen uptake means the amounts of hydrogen consumed in order to remove oxygen adsorbed on the catalysts at 773 K. In Table 4 are given the "OSC" and the dispersion state of Pd on the red-cat(A) and oxid-cat(I), as well as those in alumina-supported Pd catalyst. The effects of the structure of cerium oxides upon the catalytic activity of Pd, methane oxidation was also carried out on these Pd catalysts at 623 K, varying the partial prssure of oxygen under the constant partial pressure of methane, 1.5 kPa. The results are shown in Fig. 8.

## Discussion

**Structure of Cerium Oxides.** As can be obviously seen in Fig. 1, cerium oxides in the fresh and the oxidized cat(I) and (A) were $CeO_2$, and cerium ions in the reduced cat(I) reacted with alumina support to form $CeAlO_3$. $CeO_2$ crystallites in the fresh cat(I) were 76 Å, growing up to 132 Å in the oxidized cat(I). While in the fresh cat(A) the crystallites were as small as 33 Å and grew up to, at most, 75 Å in the oxidized cat(A) when fired at 1173 K. Thus, high dispersion of $CeO_2$ was obtained in the catalysts prepared by sol–gel method, even when the catalysts were fired at high temperatures. This is one of the features of the catalyst prepared by sol–gel method.[18] Since it was reported in our previous paper that Ni ions in dried gels prepared from tetra–ethoxy silane and nickel nitrate dissolved in ethylene glycol were dispersed in an atomic scale through Ni–O–Si bondings,[19] an atomic scale dispersion of Ce ions could be expected in the dried gels prepared from AIP sols and cerium nitrate dissolved in ethylene glycol. Thus, the atomic scale dispersion of Ce ions in the dried gels presumably resulted in the formation of tiny $CeO_2$ crystallites in the fresh cat(A).

It might be interesting to note that $CeO_2$ in the oxidized cat(I) was reversibly converted into $CeAlO_3$, when reduced in the flowing $H_2$ at 1173 K. In other words, a reversible structure change between $CeO_2$ and $CeAlO_3$ was found with an iterative reduction and oxidation at 1173 K,[20] although gradual increase in the crystallite sizes of $CeO_2$ and $CeAlO_3$ were detected with the iteration number. Since no peaks were observed in the X-ray diffraction spectrum of the reduced cat(A), structures around Ce ions could not be determined. The diffraction peaks assigned to $CeO_2$ were, however, detected, when the reduced cat(A) was fired in the flowing $O_2$ at 1173 K. This spectral change was also confirmed to be reversible; no peaks were detected when reduced by $H_2$ at 1173 K, and peaks assigned to $CeO_2$ were reversibly observed in the X-ray diffraction spectra, when fired in $O_2$ at 1173 K.

Now, the problem remained is the structures around Ce ions in the reduced cat(A). In order to discuss the problem, sample powders were subjected to EXAFS measurements, and the resulted Fourier transforms are depicted in Fig. 2, where Fourier transforms of the EXAFS spectra of pure $CeO_2$ and $CeAlO_3$ are also illustrated, for comparison. Two peaks were observed in the Fourier transform of the EXAFS spectrum of pure $CeO_2$; 1.92 Å attributed to Ce–O and 3.64 Å to Ce–Ce bonding, respectively, where phase shifts were not corrected. Two peaks were also detected at the same positions in the transforms of the EXAFS spectra of the oxidized cat(I) and (A), although the peak intensities were rather weak comparing to those of pure $CeO_2$. This indicates that the cerium oxides in the oxidized cat(I) and (A) were tiny $CeO_2$ crystallites, as already characterized by XRD. Two peaks were also recognized in the transforms of the EXAFS spectra of pure $CeAlO_3$ and the reduced cat(I); 2.81 Å ascribed to Ce–O and 3.61 Å to Ce–Al bonds in $CeAlO_3$ crystallites, respectively, being evidential of the formation of $CeAlO_3$ crystallites in the reduced cat(I). However, no reliable signals were recognized in the Fourier trans-

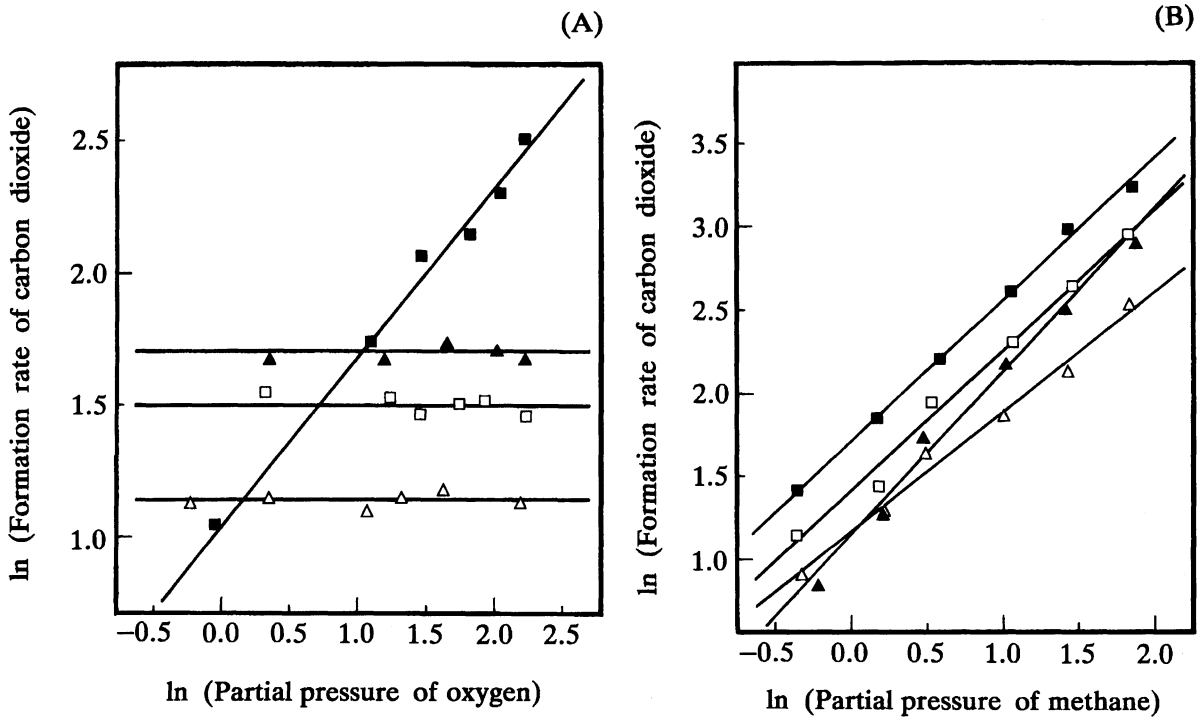


Fig. 5. (A); Change in the reaction rate with the partial pressure of oxygen at 773 K. (■); red-cat(A), (▲); red-cat(I), (□); oxid-cat(A), and (△); oxid-cat(I). (B); Change in the reaction rate with the partial pressure of methane at 773 K. (■); red-cat(A), (▲); red-cat(I), (□); oxid-cat(A), and (△); oxid-cat(I).

Table 2. Kinetic Parameters for the Methane Oxidation on Cerium Oxides at 773 K Using Gases Composed of $P_{CH_4}=1.5$ kPa and $P_{O_2}=5.3$ kPa

| Catalysts | Rate=d[$CO_2$]/d$t$ $\mu$mol-$CO_2$ $min^{-1}$ $g^{-1}$ | Rate constant $k$/$min^{-1}$ | Kinetic order | |
|---|---|---|---|---|
| | | | $m$ | $n$ |
| Oxid-cat(A) | 4.70 | 0.575 | 0.8 | 0.0 |
| Red-cat(A) | 6.33 | 0.089[a)] | 0.9 | 0.6 |
| Oxid-cat(I) | 4.22 | 0.701 | 0.7 | 0.0 |
| Red-cat(I) | 5.06 | 0.436 | 1.0 | 0.0 |

a) means that the rate constant is expressed in terms of "$mol^{-1/2}$ $min^{-1}$".

Table 3. Change in the Rate Constants with the Reaction Temperature, and the Resulting Activation Energies on Various Cerium Oxide Catalysts

| Catalysts | Rate constant $k$/$min^{-1}$ | | | | | Activation energy |
|---|---|---|---|---|---|---|
| | 673 | 723 | 773 | 823 | 873 | kcal $mol^{-1}$ |
| Oxid-cat(A) | 0.054 | 0.141 | 0.575 | 1.175 | 3.767 | 24.6 |
| Red-cat(A) | 0.002[a)] | 0.016[a)] | 0.089[a)] | 0.213[a)] | 0.436[a)] | 29.8 |
| Oxid-cat(I) | 0.045 | 0.157 | 0.701 | 1.612 | 2.369 | 24.2 |
| Red-cat(I) | 0.030 | 0.144 | 0.436 | 0.725 | 2.705 | 24.8 |

Gasses employed are the same as noted in Table 2.
a) means the same as in Table 2.

form of the EXAFS spectrum of the reduced cat(A). This suggests at least, two possibilities for the structure around Ce ions in the reduced cat(A): One is that the Ce ions were still dispersed in the bulk alumina in an atomic scale with random Ce–O bond lengths, where distinct signals might be expected neither in the XRD spectra nor in the EXAFS Fourier transforms. The other possibility is that the cerium ions coagulated to form several kinds of nonstoichiometric cerium oxides, $CeO_{2-x}$, in the reduced cat(A), since there have been reported a plenty of $CeO_{2-x}$ species stabilized in a reducing atmosphere.[10,21)] The Ce–O bond lengths in the $CeO_{2-x}$ species are somewhat different with each other, suggesting that various Ce–O bond lengths were

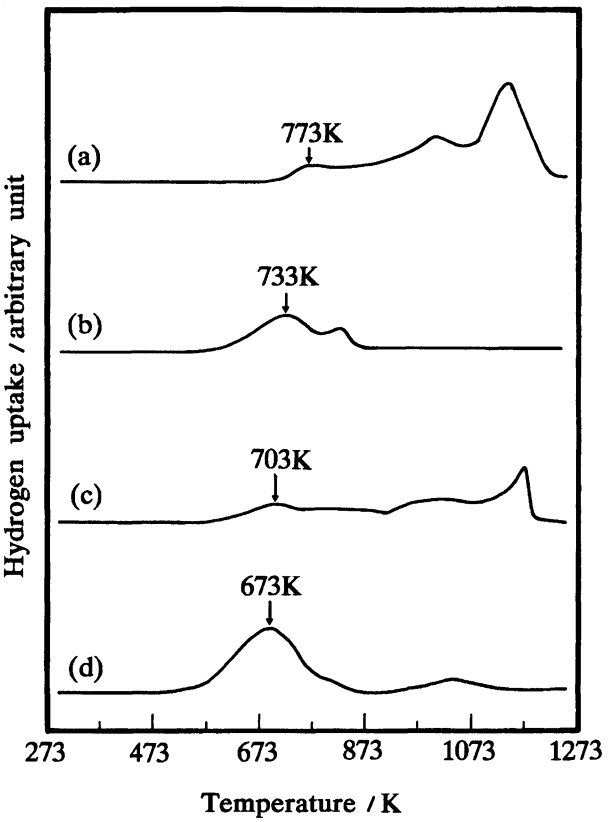


Fig. 6. TPR spectra of oxygen adsorbed at 773 K on (a); oxid-cat(I), (b); red-cat(I), (c); oxid-cat(A), and (d); red-cat(A).

formed in the reduced cat(A). This deplettes the peak intensity, which should be assigned to a Ce–O bonding, in the Fourier transform of the reduced cat(A). No peaks in the XRD spectra will be well explained by the formation of finely-divided $CeO_{2-x}$ crystallites in the reduced cat(A).

Fluorescence measurements are the best to discuss whether atomic scale dispersions or finely-divided $CeO_{2-x}$ crystallites were in the reduced cat(A). It is well known that the fluorescent intensity of metal ions increases with an increase in the number of metal ions dispersed in an atomic scale, and that the intensity begins to decrease, in turn, when the concentration of metal ions is too much. This is so called a concentration quenching of florescence, caused by the interaction between the metal ions intimately located. Coagulation of the metal ions always induces the quenching of the fluorescence and, in this sense, the results given in Fig. 3 support the coagulation of cerium ions to form finely-divided $CeO_{2-x}$ crystallites in the reduced cat(A). Consequently, the structure of cerium oxides, as well as the reversible structural changes, in the catalysts prepared in this work are summarized, as illustrated in Fig. 7.

**"OSC" and Methane Oxidation.** The structure of cerium oxides in the catalysts were reflected on the "OSC" values, expressed in terms of mmol of $O_2$ per mol of $CeO_2$, as shown in Fig. 4. The increase in the "OSC" with an elevation of the temperature implies that lattice oxygens, as well as the adsorbed oxygens, in the cerium oxides play an important role for the "OSC". It has been reported that the "OSC" is principally originated in the diffusion of lattice oxygen and the oxygen vacancies in the cerium oxide crystallites.[17,22] In the present work, the "OSC" was measured by the cyclic pulsing of 1 vol% $O_2$/He and 2 vol% $H_2$/He at every two min,[17] so that only the lattice oxygen and the oxygen vacancies at the surface vicinities of the crystallites could participate to enhance the "OSC". Therefore, no structural change in the bulk crystallites were recognized in the XRD spectra between before and after the "OSC" measurements. The results given in Fig. 4 show a decrease in the "OSC" value in the following sequence; red-cat(A)>red-cat(I)>oxid-cat(A)>oxid-cat(I), in other words, finely-divided $CeO_{2-x}$>$CeAlO_3$>small-sized $CeO_2$>large $CeO_2$ crystallites. It might be reasonable that there are considerable amounts of oxygen vacancies in the cerium oxides treated in the flowing $H_2$, comparing to those treated in the flowing $O_2$. This resulted in the higher "OSC" for the reduced cat(A) and (I) than for the oxidized cat(A) and (I). Considering the $CeO_2$ crystallite sizes, given in Table 1, the surface area of $CeO_2$ crystallites in the oxid-cat(A) will be larger than that in the oxid-cat(I), leading to the higher "OSC" of the former. If a complete redox cycle is assumed for the reaction,

$$2CeO_2 \rightleftharpoons Ce_2O_3 + 1/2O_2, \quad (1)$$

the amounts of oxygen reversibly absorbed and released ("OSC") are 250 mmol $O_2$ per mol of $CeO_2$. The "OSC" observed in this work was, at most, 50 mmol of $O_2$ for the reduced cat(A), suggesting that the lattice oxygen or the oxygen vacancies existing in a thin surface layer, ca. 2.5 Å below the surface of $CeO_2$ crystallites (75 Å, see Table 1), could participate to the "OSC" under the conditions employed. The "OSC" at 773 K, where the methane oxidation was carried out, was less than 5 mmol of $O_2$ per mol of $CeO_2$ for the catalysts used, which means that oxygen vacancies located just on the surface of the crystallites could participate to "OSC" at 773 K.

The kinetic parameters obtained for methane oxidation at 773 K over these cerium oxide catalysts are summarized in Table 2, where the first order kinetics with respect to methane and zero order kinetics with respect to oxygen on all the catalysts, except the reduced cat(A), are informed, i.e., $[\text{rate}] = kP_{CH_4}{}^1P_{O_2}{}^0$. Similar rate equations have already been reported on noble metal catalysts such as Pt, Pd and Rh,[23—25] although the reaction order with respect to partial pressure of oxygen was not always zero, depending on the ratio of $P_{O_2}/P_{CH_4}$ and on the dispersion states of the metals.[26,27] The equation above suggests an Eley–Rideal mechanism for the methane oxidation over

Table 4. "OSC" and the Pd Particle Sizes on the Cerium Oxide/Alumina Catalysts

| Catalysts | Oxygen storage capacity (OSC) | | Pd dispersion | Pd particle size/Å |
|---|---|---|---|---|
| | $\mu$mol-$O_2$ g-cat$^{-1}$ | mmol-$O_2$ mol-$CeO_2^{-1}$ | | |
| $Pd/Al_2O_3$ | 0.99 | — | 0.03 | 260 |
| Oxid-cat(I) | 0.07 | 0.06 | — | — |
| Pd/oxid-cat(I) | 8.06 | 6.94 | 0.03 | 290 |
| Red-cat(A) | 1.34 | 1.15 | — | — |
| Pd/red-cat(A) | 37.39 | 32.09 | 0.10 | 90 |

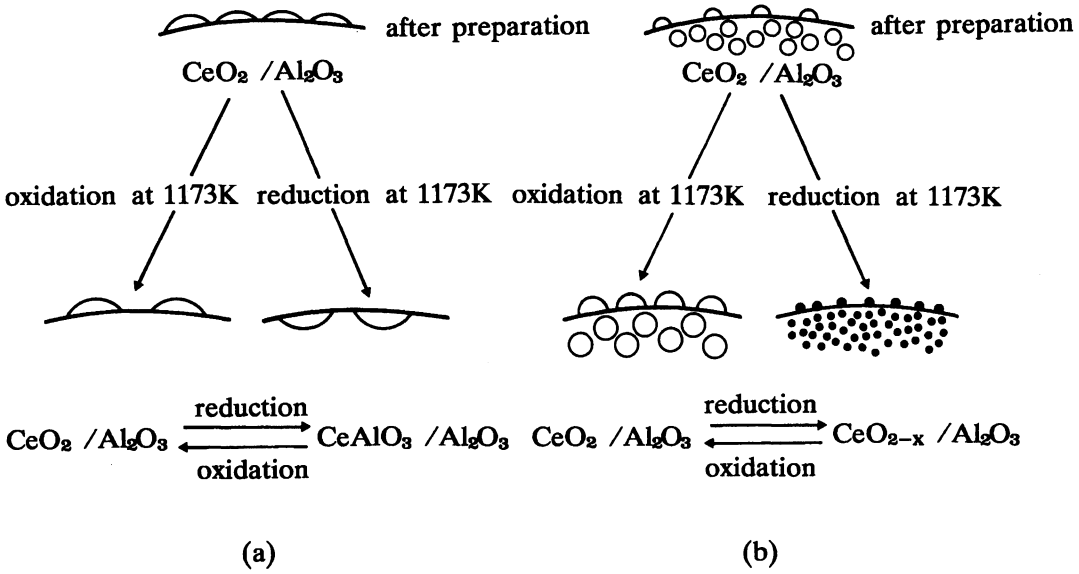


Fig. 7. A schematic model for the reversible structure change in cerium oxides. (a); catalysts by impregnation method, (b); catalysts by sol–gel method.

cerium oxide catalysts, though Otto has suspected the mechanism on alumina-supported platinum catalysts and claimed that the rate controlling step might be in the dissociation of methane on Pt.[27] While on the reduced cat(A) the reaction order of oxygen was found not to be zero, and the rate can be expressed as follows; $[\text{rate}]=kP_{CH_4}{}^{1}P_{O_2}{}^{0.5}$, indicating that the interaction between dissociatively adsorbed oxygen and methane are important for the progress in the oxidation reaction. One of the possible mechanisms, which will satisfy the equation above, is as follows;

$$2O_2(g) + 4\text{-s} \rightleftharpoons 4\text{O-s} \quad (2)$$

$$CH_4(g) + \text{O-s} \rightarrow CH_2\text{-s} + H_2O(g) \quad (3)$$

$$CH_2\text{-s} + 3\text{O-s} \rightarrow CO_2 + H_2O(g), \quad (4)$$

where "s" represents the oxygen vacancies, on which oxygen adsorbs from gas phase. Recently, Li et al.[28] have reported that there are, at least, two kinds of adsorption sites on cerium oxides for oxygen adsorption; one is the coordinately unsaturated $Ce^{4+}$ and the other is $Ce^{3+}$ formed by oxygen defects at the surface. Oxygens adsorbed on $Ce^{4+}$ were characterized to be $O_2^-$, and the oxygens adsorbed on $Ce^{3+}$ were to be $O_2^{2-}$, respectively, by infrared spectroscopy.[28] Considering that there are much amounts of $Ce^{3+}$ on the surface of $CeO_{2-x}$, adsorbed $O_2^{2-}$ species are predominant on the finely-divided $CeO_{2-x}$ catalysts, while $O_2^-$ species are dominantly produced on the surface of $CeO_2$ catalysts. Although both dioxygen species were converted into $O^-$, and finally into lattice oxygen ($O^{2-}$), by accepting more electrons from the surface, there should be some differences in the reactivity toward methane between $O^-$ on $Ce^{4+}$ and $O^-$ on $Ce^{3+}$. As will be mentioned below, the TPR spectrum of the finely-divided $CeO_{2-x}$ was much different from that of the $CeO_2$ catalyst, suggesting the difference in the reactivity of $O^-$ on $Ce^{4+}$ from that on $Ce^{3+}$. The results obtained in the present work seem to indicate that $O^-$ on $CeO_2$ reacted with gaseous methane to form $CO_2$ and $H_2O$ according to the Eley–Rideal mechanism, and the $O^-$ over the finely-divided $CeO_{2-x}$ produced adsorbed $CH_2$-s as a reaction intermediate, which might be a rate controlling step of the methane oxidation on the red-cat(A). Trimm and Lam[26] are of the opinion that methane fragments, $CH_x$-s, produced over $Pt/Al_2O_3$ catalyst are the reaction intermediate, when the methane oxidation was carried out at the temperatures higher than 810 K. They also mentioned that methane competitively adsorbed on Pt with oxygen at higher temperatures, and that

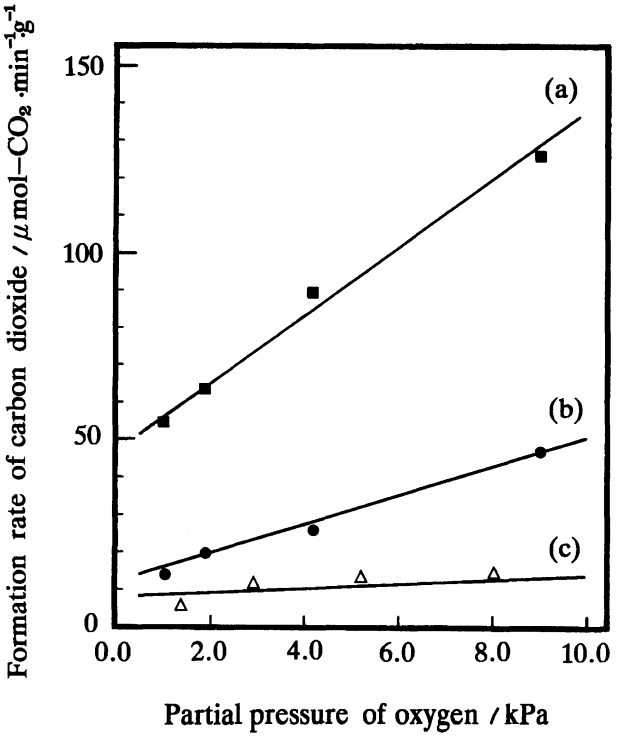


Fig. 8. The rate of methane oxidation on (a); Pd/red-cat(A), (b); $Pd/Al_2O_3$, (c); Pd/oxid-cat(I). Reaction was carried out at 623 K.

the activation energy for methane oxidation decreased at the temperatures higher that 810 K. Otto[27] has also reported the decrease in the activation energy for methane oxidation on $Pt/Al_2O_3$ when Pt loading was more than 10 wt%, and has claimed the possibility of adsorbed hydrocarbon, $CH_x$-s, as a reaction intermediate.

As can be seen in Table 3, the activation energies for the methane oxidation on the oxid-cat(I) and (A) and on the red-cat(I) were almost the same (ca. 25 kcal $mol^{-1}$), while on the red-cat(A) the activation energy was rather higher (ca. 30 kcal $mol^{-1}$). This also indicates that the reaction mechanism on the red-cat(A), consisting of finely-divided $CeO_{2-x}$, might be different from those on the other cerium oxide catalysts.

**Characterization of Oxygen Adsorbed on Cerium Oxides by TPR.** Since the relationship between the "OSC" and the activity for methane oxidation is still ambiguous in the discussion above, oxygen adsorbed on the cerium oxides at 773 K was studied by TPR measurements (see Fig. 6). Three peaks were observed for the adsorbed oxygen on the oxid-cat(I); two tiny peaks centered around 773 and 1023 K, respectively, and a strong peak at 1143 K. The first two peaks have been assigned to the oxygen adsorbed at the surface or the surface vicinities of $CeO_2$ crystallites.[2] The third peak was assigned to the oxygen located at the interfaces between $CeO_2$ crystallites and alumina, and the appearance of this peak is an evidence of the formation of $CeAlO_3$.[20] Similar spectrum was obtained for the oxygen adsorbed on the oxid-cat(A), where weak and broad peaks were recorded at 703 and 1023 K, respectively, and a strong peak at 1173 K. These peaks were assigned in the same manner as those on the oxid-cat(I). While on the red-cat(I), consisting of $CeAlO_3$ crystallites, relatively strong peaks were detected only at 733 and 823 K, and on the red-cat(A), consisting of finely-divided $CeO_{2-x}$, a strong peak at 673 K and a broad peak around 1023 K were observed. Since the methane oxidation was carried out at 773 K, the reduction peaks observed at temperatures lower than 773 K should be discussed to reveal the relationship between "OSC" and the catalytic activities. Apparently, the peak area below 773 K decreased in the sequence of red-cat(A)>red-cat(I)>oxid-cat(A)>oxid-cat(I), which is consistent with the decreasing order of "OSC" at 773 K (see Fig. 4) and with the decreasing order of the activity for the methane oxidation at 773 K (see Table 2). Consequently, it might be natural to conceive that the oxygen of "OSC" originates in the oxygen adsorbed on the oxygen vacancies at the surface of the cerium oxide crystallites. Some parts of the adsorbed oxygen migrate into the bulk crystallites to be the lattice oxygen and the other parts stay there to react with methane;

$$O_2(g) + 2\text{-s} \rightleftharpoons 2O^-\text{-s} \rightarrow 2O^{2-}\text{-l}, \quad (5)$$

where $O^{2-}$-l is the oxygen migrated into the bulk crystallites and is hard to be released. The rate of migration into the bulk is a function of the temperatures and, as can be seen in Fig. 4, the "OSC" increased with an increase in the temperatures, which suggests that the "OSC" includes both O-s and O-l. At temperatures around 773 K, the rate of migration into the bulk will be so low that the oxygen in the "OSC" could be considered to be the adsorbed oxygen ($O^-$-s) which reacts with methane to $CO_2$ and $H_2O$. On the red-cat(A), the adsorbed oxygen ($O^-$-s) was removed by $H_2$ at 673 K, while on the other catalysts it requested the temperatures higher than 700 K, suggesting that the oxygen vacancies in the finely-divided $CeO_{2-x}$ more weakly adsorb oxygen than those in the other cerium oxides, which will cause the differences in the reaction mechanism of, and subsequently, in the activation energy for methane oxidation on finely-divided $CeO_{2-x}$ catalyst and on the other cerium oxides.

**"OSC" and Methane Oxidation on Supported Pd Catalysts.** In order to study the effects of cerium oxides upon the catalytic behavior of Pd in ceria/alumina-supported Pd catalysts, the "OSC" and the rate of methane oxidation on Pd/oxid-cat(I) and Pd/red-cat(A), as well as on $Pd/Al_2O_3$, were measured. The average sizes of Pd in these catalysts, measured by CO chemisorption at room temperature, were 250 Å for $Pd/Al_2O_3$ and Pd/oxid-cat(I), 100 Å for Pd/red-cat(A), respectively. The "OSC" for $Pd/Al_2O_3$ cata-

lyst is the amount of $O_2$ reversibly adsorbed and desorbed on Pd according to the following redox reaction; $O_2(g)+2Pd \rightarrow 2PdO$, and $PdO+H_2 \rightarrow Pd+H_2O(g)$. The "OSC" for $Pd/Al_2O_3$ shown in Table 4, 0.99 μmol $O_2$/g-cat, indicates that more than 70% of the surface Pd atoms are oxidized to PdO during the redox reaction. While on the oxid-cat(I) and the red-cat(A), the "OSC"s are significantly enhanced to be 6.94 and 37.29 μmol $O_2$/g-cat., respectively, which are much higher than the total "OSC" of "$Pd/Al_2O_3$ and oxid-cat(I)" and of "$Pd/Al_2O_3$ and red-cat(A)," respectively. One of the possible ideas to explain this result is an oxygen spill-over from Pd on to the cerium oxides; oxygen in the gas phase is first activated on the surface of Pd, and then moved over the surface of cerium oxides according to the following mechanism;

$$O_2(g) + 2Pd \rightleftharpoons 2PdO \quad (6)$$

$$PdO + \text{-s} \rightleftharpoons Pd + \text{O-s}, \quad (7)$$

where -s means the sites for oxygen adsorption on cerium oxides. Thus, the role of Pd in these catalysts are the dissociation or activation of gaseous oxygen to readily spill over to the cerium oxides, although the cerium oxides are of poor potential to activate the gaseous oxygen by themselves. The "OSC" strongly depends on the cerium oxides used, and on the Pd/oxid-cat(I), the oxygen moved on to the cerium oxides is speculated to be strongly bounded to $CeO_2$, from the TPR spectrum in Fig. 6. While on the Pd/red-cat-(A), the oxygen spilled over the cerium oxides is conceived to be weakly trapped at the oxygen vacancies of $CeO_{2-x}$ (see also the TPR spectrum in Fig. 6) so as to be easily released into gas phase or to move on to the alumina surface. Consequently, the number of oxidized Pd atoms during the redox reaction is significantly dependent upon the cerium oxides employed; the amount of oxidized Pd atoms decreases in the Pd/red-cat(A), and increases in the Pd/oxid-cat(I). Hence, the catalytic activity of Pd catalysts for methane oxidation was suppressed on the Pd/oxid-cat(I), and, conversely, significantly enhanced on the Pd/red-cat(A), shown in Fig. 8. The enhancement in the activity of Pd/red-cat-(A) for methane oxidation could not be explained only by the difference in the Pd particle sizes; 250 and 100 Å for Pd/oxid-cat(I) and Pd/red-cat(A), respectively. It must be mentioned that the reaction order of oxygen on the Pd/red-cat(A) was 0.4, while that on the Pd/oxid-cat(I) was less than 0.1. These correspond to the reaction order of oxygen on the red-cat(A) and on the oxid-cat(I); 0.5 and 0, respectively, as mentioned previously. Although it is still ambiguous to elucidate the difference in the reaction mechanism on Pd/red-cat(A) and Pd/oxid-cat(I), the adsorbed hydrocarbon species, expressed by $CH_x$-s, on Pd or on the finely-divided $CeO_{2-x}$ are tentatively proposed to be a reaction intermediate during the methane oxidation on the Pd/red-cat(A).

The authors express their thanks to Institute for Molecular Science at Okazaki, for the measurements of fluorescent spectra, and the measurements and analysis of EXAFS data.

## References

1) "Kagaku- Binran, Kisohen II," ed by Japanese Chemical Society, Maruzen, Tokyo (1984), p. II-476 (in Japanese).
2) H. Yao and Y. F. Yu-Yao, *J. Catal.*, **86**, 254 (1984).
3) G. Kim, *Ind. Eng. Chem. Prod. Rev. Dev.*, **21**, 267 (1982).
4) H. S. Gandhi and M. Shelef, *Stud. Surf. Sci. Catal.*, **30**, 199 (1987).
5) R. K. Herz and J. A. Sell, *J. Catal.*, **94**, 166 (1985).
6) J. T. Kummer, Y. F. Yu-Yao, and D. McKee, "Proceedings of American Engineering Congress," Detroit, Michi., 1976, Abstr., No. 760143.
7) Y. F. Yu-Yao, *Ind. Eng. Chem. Prod. Res. Dev.*, **19**, 293 (1980).
8) S. H. Oh and C. C. Eickel, *J. Catal.*, **112**, 543 (1988).
9) J. C. Summers and S. A. Ausen, *J. Catal.*, **58**, 131 (1979).
10) D. J. M. Beavan, *J. Inorg. Nucl. Chem.*, **1**, 49 (1955).
11) Kh. M. Minachev, "Proceedings of 5th Int. Congr. Catal.," North-Holland (1973), p. 219.
12) T. Hattori, J. Inoko, and Y. Murakami, *J. Catal.*, **42**, 60 (1976).
13) K. Ishiguro, T. Ishikawa, N. Kakuta, A. Ueno, M. Mitarai, and T. Kamo, *J. Catal.*, **123**, 523 (1990); T. Ishikawa, R. Ohashi, H. Nakabayashi, N. Kakuta, A. Ueno, and A. Furuta, *J. Catal.*, **134**, 87 (1992).
14) T. Mizushima, K. Tohji, Y. Udagawa, and A. Ueno, *J. Am. Chem. Soc.*, **94**, 4980 (1990).
15) K. Tohji, Y. Udagawa, S. Tanabe, and A. Ueno, *J. Am. Chem. Soc.*, **106**, 612 (1984).
16) R. Morimo, T. Mizushima, Y. Udagawa, N. Kakuta, A. Ueno, and H. Namikawa, *J. Electrochem. Soc.*, **137**, 2340 (1990).
17) T. Miki, T. Ogawa, M. Haneda, N. Kakuta, A. Ueno, S. Tateishi, S. Matsuura, and M. Sato, *J. Phys. Chem.*, **94**, 6464 (1990).
18) A. Ueno, H. Suzuki, and Y. Kotera, *J. Chem. Soc., Faraday Trans. 1*, **79**, 127 (1983).
19) A. Ueno, "Hyoumen-no-Kagaku (Surface Science)," ed by K. Tamaru, Gakkai-Syuppan Pub. Co., Tokyo (1985), p. 327 (in Japanese).
20) T. Miki, T. Ogawa, N. Kakuta, A. Ueno, S. Matsuura, and M. Sato, *Chem. Lett.*, **1988**, 565.
21) G. Rienacker and M. Birckenstadet, *Z. Anorg. Chem.*, **265**, 99 (1951).
22) T. Jin, T. Okuhara, G. J. Mains, and J. M. White, *J. Phys. Chem.*, **91**, 3310 (1987).
23) C. Kemball and W. R. Patterson, *Proc. R. Soc. London, Ser. A*, **1962**, 270, 219.
24) W. R. Patterson and C. Kemball, *J. Catal.*, **2**, 465 (1963).
25) M. Niwa, K. Awano, and Y. Murakami, *Appl. Catal.*,

**7**, 317 (1983).
26) D. L. Trimm and C. W. Lam, *Chem. Eng. Sci.*, **35**, 1405 (1980).
27) K. Otto, *Langmuir*, **5**, 1364 (1989).
28) C. Li, K. Domen, K. Maruya, and T. Onishi, *J. Am. Chem. Soc.*, **111**, 7683 (1989).